

The University of Wisconsin Arctic High-Spectral Resolution Lidar: General Information and Data Examples

Gijs de Boer, Edwin Eloranta

The University of Wisconsin – Madison, Madison, WI USA

1. Introduction

The University of Wisconsin Arctic High-Spectral Resolution Lidar (UW-AHSRL; Eloranta, 2005) has acquired months of continuous measurements in two high Arctic locations. A similar deployment to Antarctica would provide both an interesting contrast as well as practical analysis tool in the study of high-latitude precipitation and clouds. In addition to the measurements made by the lidar, the instrument has also been co-located with a NOAA ETL Millimeter Cloud Radar to establish a long-range data set of cloud microphysical property retrievals. These properties include effective particle size, number density and water content. Discussed in this paper are measurements and practical specifications for the AHSRL, examples of data, an explanation of the combined retrieval algorithms, and an overview of data accessibility on our web-server.

2. The University of Wisconsin Arctic High-Spectral Resolution Lidar

a) Technical Specifications

The AHSRL was designed to run unattended in remote locations. A general overview of system specifications and operating requirements is given in table 1. The lidar requires some sort of protective housing with a glass window built into the ceiling. This glass should be heated and sloped to aid in snow and water removal. The housing should be temperature controlled and held within the 60-75 degree Fahrenheit range.

The system transmits at a wavelength of 532 nm and average power of 0.6 W, making it eye-safe. The 40 cm receiver is designed to reduce the effects of multiple scattering through the use of a small angular field of view (45 μ rad). Obtainable range resolution is as high as 7.5 meters, with a maximum time resolution of 0.5 seconds. Normally, some averaging is done to reduce noise. The system has an observational range of 75m-35km from the system, with a maximum observable optical depth of around 4.

b) Previous Deployments

To date, the AHSRL has been deployed to two separate Arctic locations. The first deployment took place in the fall of 2004 as a part of the Mixed-Phase Arctic Clouds Experiment (M-PACE; Verlinde et al., 2007). The AHSRL was located at Point Barrow, AK for approximately 2 months during which it collected nearly continuous data. The second deployment is currently ongoing. Since the summer of 2005, the AHSRL has been in Eureka, Canada as a part of the Study of Environmental Arctic Change (SEARCH) campaign. At both locations, the lidar has run unattended. Control of the system is accomplished via a network connection, and all data is streamed to our laboratories in Madison, WI. From here, the data is posted to the website in near real

REQUIREMENTS		DESCRIPTION	
Power:	120V, 30A	Wavelength:	532 nm
Network:	~16 kb/s avg.	Power:	0.6 W
Space:	82"x120"	Rep. Rate:	4 kHz
Window:	18" Tilted ceiling window	Beam Divergence:	10 μ rad
Temperature:	60-75 F	Field of View:	45 μ rad
		Range Resolution:	7.5 m (min)
		Time Resolution:	0.5 s (min)
		Maximum observable optical depth:	~4

Table 1: System requirements and technical description.



Figure 1: The AHSRL (left) and its current housing in Eureka (right).

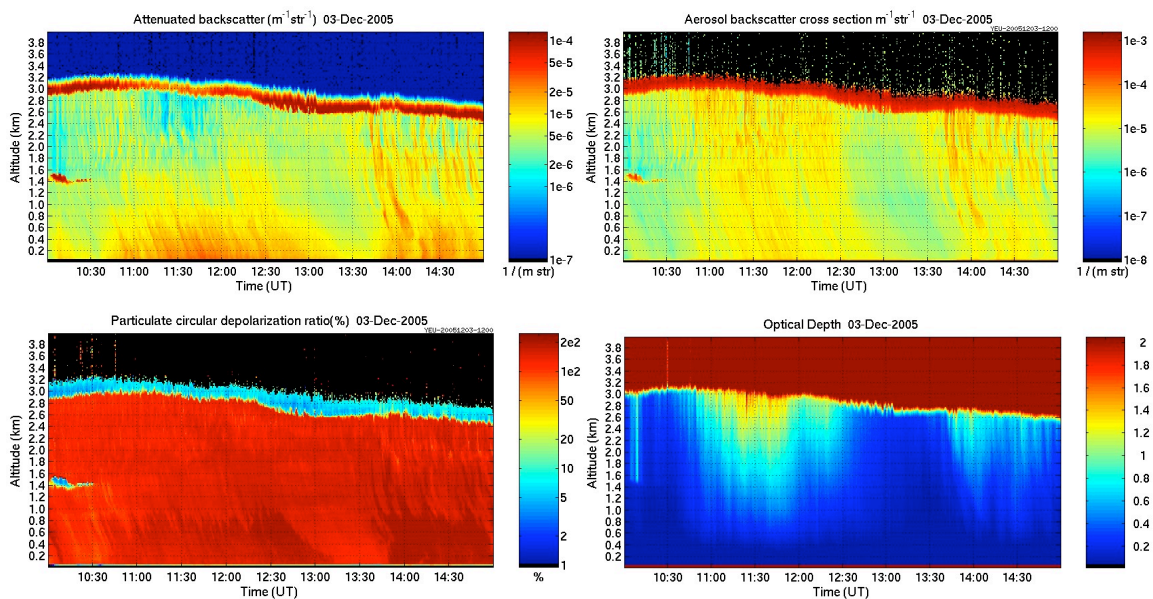


Figure 2: Data examples, clockwise from top-left, of attenuated lidar backscatter, calibrated aerosol backscatter cross-section, calibrated optical depth, and particle depolarization ratio. These examples show a thin, mixed-phase, boundary layer cloud.

time. For the extended Eureka deployment, a quarterly site visit has been performed to adjust and clean hardware components. At both sites, the AHSRL was collocated with a NOAA Millimeter Cloud Radar (MMCR) inside a climate-controlled sea-container (figure 1).

c) Measurements and Data Examples

Unlike traditional lidar systems, an HSRL does not require assumptions about molecular attenuation. Using a molecular channel for reference purposes, the AHSRL provides absolutely calibrated measurements of aerosol backscatter cross-section, depolarization and optical depth, in addition to traditional backscatter profiles (figure 2).

3. Microphysical Retrievals

a) Overview of Techniques

The retrieval algorithms used are very similar to those used by Donovan and Van Lammeren (2001). From the lidar and radar backscatter cross-section, particle effective size, particle number density and water content are derived. Because the AHSRL is able to provide absolutely calibrated measurements of scattering cross-section, a priori assumptions are not necessary to correct for attenuation, as they were in previous applications of this technique.

b) Particle Effective Size

For a distribution of particles, the radar scattering cross-section is equal to:

$$\beta_{rad} = \frac{24\pi^3 k^2}{\lambda^4} \langle V^2 \rangle \quad (1)$$

where k^2 is the dielectric constant, λ the radar wavelength, and $\langle V^2 \rangle$ the average volume squared. The lidar scattering cross-section is equal to:

$$\beta_{lid} = 2\langle A \rangle \quad (2)$$

where $\langle A \rangle$ is the average area of the particle distribution.

Using a backscatter phase function for both signals, backscatter cross-sections can be used in a ratio to come up with this expression:

$$\frac{\frac{P(180)}{4\pi} \beta'_{rad}}{\frac{3}{8\pi} \beta'_{lid}} = \frac{12\pi^3 k^2}{\lambda^4} \frac{\langle V^2 \rangle}{\langle A \rangle} \quad (3)$$

where β' is now the backscatter cross-section. Using the definition for effective radius:

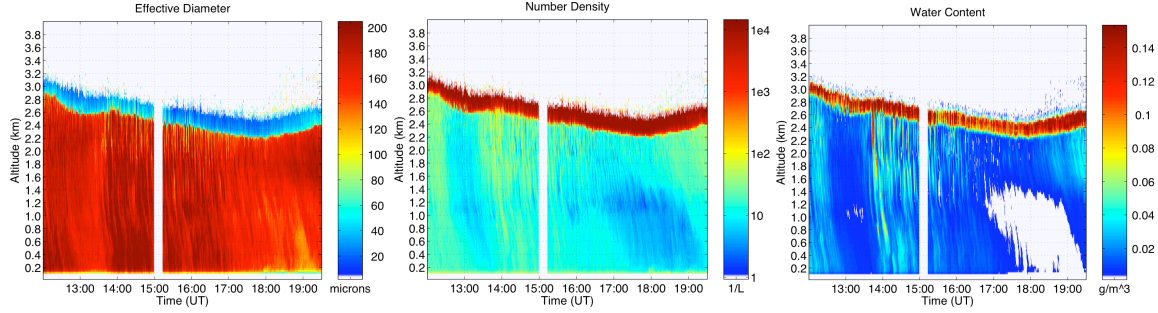


Figure 3: Examples of microphysical retrievals using the AHSRL and MMCR. From left, particle effective diameter, particle number density, and water content. Observed here is the same case from figure 2, with a mixed phase cloud layer, precipitating ice.

$$r_{eff} = \frac{\pi}{\frac{4}{3}\pi} \frac{\langle V \rangle}{\langle A \rangle} \quad (4)$$

equation (3) becomes:

$$\frac{\frac{P(180)}{4\pi}}{\frac{3}{8\pi}} \frac{\beta'_{rad}}{\beta'_{lid}} = \frac{16\pi^3 k^2}{\lambda^4} r_{eff} \frac{\langle V^2 \rangle}{\langle V \rangle} \quad (5)$$

This expression can be solved for effective radius, assuming an expression for the volume of a particle and integrating over a distribution. In this study, a modified gamma distribution was utilized, and the volume of a particle is defined as:

$$V = \sigma_V \frac{\pi}{6} D_{ref}^{3-\delta_V} D^{\delta_V} \quad (6)$$

where σ_V and δ_V are user supplied parameters, and are equal to 1 and 3 respectively for water.

c) Particle Number Density

The amount of particles in the scattering volume is related to the backscatter cross-section as follows:

$$N = \frac{\beta'_{lid}}{2 \left(\frac{P(180)}{4\pi} \right) \langle A \rangle} \quad (7)$$

d) Water Content

Having an estimate for the number of particles and their size allows for an estimate of water content:

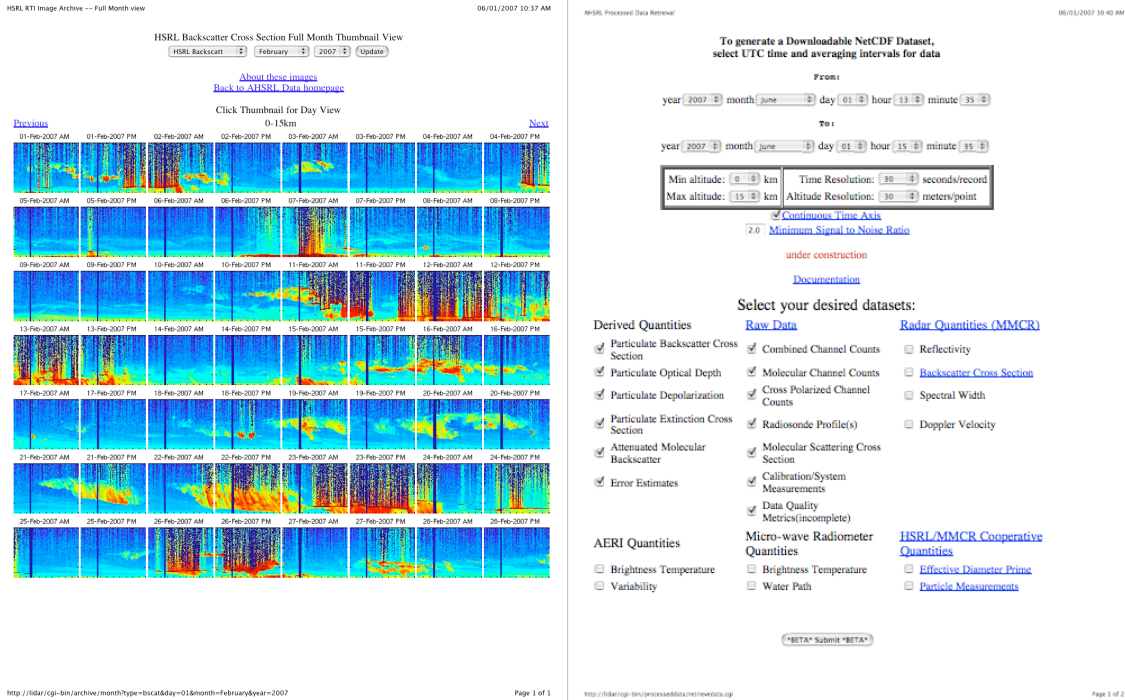


Figure 4: Examples of the data website. The left image displays one entire month's worth of data, while the right image displays the netcdf creation page. User-defined height and time scales can be used to create images, as shown in figures 2 and 3.

$$WC = \frac{2}{3} D_{eff} \langle A \rangle N \rho_{ice} \quad (8)$$

e) Validation

These retrieval methods are continually compared to aircraft measurements to test their accuracy. Although several assumptions are required for both frozen and mixed precipitation, estimated quantities fall within reasonable ranges, and show vertical and horizontal patterns similar to those seen in the aircraft data. The largest errors come as a result of improper selection of ice habit type in formulating volume and area power-law estimates.

4. Data Acquisition and Sharing

All of the data that is collected by the AHSRL is publicly available on our website at <http://lidar.ssec.wisc.edu>. Examples of this site are shown in figure 4. Lidar data from altitudes below 15km are posted in near-real time, while higher data is transferred monthly and available upon request. In addition to the AHSRL data, measurements made by the collocated MMCR and AERI instruments are also presented. Quick look images show all data from one month on a single web page. In addition, the site user can select the averaging interval, height and time ranges, as well as what data they would like to see. In addition to viewing the data online, users can download netcdf files containing all

of the data, as well as the microphysical retrievals.

5. References

- Donovan, D.P. and A.C.A.P. van Lammeren, 2001: Cloud Effective Particle Size and Water Content Profile Retrievals Using Combined Lidar and Radar Observations I: Theory and Examples. *J. Geophys. Res.* **106**, 27425-27488.
- Eloranta, E. W., I. A. Razenkov, R. E. Kuehn, R. E. Holz, J. P. Hedrick, and J. P. Garcia, A High Spectral Resolution Lidar for Operation in the Arctic. *Atmospheric Radiation Measurement (ARM) Program Science Team Meeting*, April 8-11, St Petersburg, FL.
- Verlinde, J., J. Y. Harrington, G. M. McFarquhar, V. T. Yannuzzi, A. Avramov, S. Greenberg, N. Johnson, G. Zhang, M. R. Poellot, J. H. Mather, D. D. Turner, E. W. Eloranta, B. D. Zak, A. J. Prenni, J. S. Daniel, G. L. Kok, D. C. Tobin, R. Holz, K. Sassen, D. Spangenberg, P. Minnis, T. P. Tooman, M. D. Ivey, S. J. Richardson, C. P. Bahrmann, M. Shupe, P. J. DeMott, A. J. Heymsfield, and R. Schofield, 2007: The Mixed-Phase Arctic Cloud Experiment, *Bull. Am. Met. Soc.*, **88**, 205-221.